

Analysis of Bivariate Jump-Diffusion Processes

Leonardo Rydin Gorjão,^{1,2,3,4,*} Jan Heysel,^{1,2,†} Klaus Lehnertz,^{1,2,5,‡} and M. Reza Rahimi Tabar^{6,7,§}

¹Department of Epileptology, University of Bonn, Venusberg Campus 1, 53127 Bonn, Germany

²Helmholtz Institute for Radiation and Nuclear Physics, University of Bonn, Nussallee 14–16, 53115 Bonn, Germany

³Institute for Theoretical Physics, University of Cologne, 50937 Köln, Germany

⁴Forschungszentrum Jülich, Institute for Energy and Climate Research - Systems Analysis and Technology Evaluation (IEK-STE), 52428 Jülich, Germany

⁵Interdisciplinary Centre for Complex Systems, University of Bonn, Brühler Straße 7, 53175 Bonn, Germany

⁶Institute of Physics and ForWind, Carl von Ossietzky University of Oldenburg, Carl-von-Ossietzky-Straße 9–11, 26111 Oldenburg, Germany

⁷Department of Physics, Sharif University of Technology, 11365-9161, Tehran, Iran

We introduce the bivariate jump-diffusion process, comprising two-dimensional diffusion and two-dimensional jumps, that can be coupled to one another. We present a data-driven, non-parametric estimation procedure of higher-order Kramers–Moyal coefficients that allows one to reconstruct relevant aspects of the underlying jump-diffusion processes and recover the underlying parameters of a jump-diffusion process. The procedure is validated with numerically integrated data using synthetic bivariate continuous and discontinuous time series. We further evaluate the possibility of estimating the parameters of the jump-diffusion model via a data driven analyses of the higher-order Kramers–Moyal coefficients, and the limitations arising from the scarcity of points in the data or disproportionate parameters in the system.

I. INTRODUCTION

Growing evidence indicates that continuous stochastic modeling of time series of complex systems (white noise-driven Langevin equation) should account for the presence of discontinuous jump components [1–10].

Examples include dynamics of charge transport in various materials [11], stochastic resonance [12], moving fronts [13], light curves of variable astronomical objects [14], fluctuations of wind and solar power systems [15], early warning signals of systems near to their tipping points [16], transitions in financial [17, 18] and climate data [19], ion channel dynamics [20] eye movements [21], or movement and foraging paths of animals [22].

Such time series have some distinct characteristics such as heavy tails and occasionally sudden large jumps. Non-parametric (data-based) modelling of time series with jumps provides an attractive way of estimating the parameters of the system given this estimations depend solely on the data available, without *ad hoc* assumptions.

Many theoretical models have been developed in the context of mathematical finance to describe discontinuous components [7]. Among them, jump-diffusion modelling provides a theoretical tool to study processes of known and unknown nature that exhibit jumps. This modelling has received attention in the literature due to the existence of non-parametric estimation procedures to uncovers the underlying parameter of the process in

examination, e.g. estimating the Kramers–Moyal coefficients [8–10]. It allows one to study the drift and diffusion of the process, as well as the intensity of the discontinuous jump component [6, 8], as well as potential non-linearities present in the process.

The focus of this paper is to introduce a method to investigate bivariate time-series with discontinuous jump components. We begin with an overview of bivariate diffusion processes that exhibits the known relation between the parameters and functions in stochastic modelling and the Kramers–Moyal coefficients. Exemplary processes are portrayed, and we propose a measure to judge the quality of our reconstruction procedure. We then present bivariate jump-diffusion processes alongside with the associated Kramers–Moyal expansion, and investigate the suitability of our reconstruction procedure using various examples. We conclude this paper by summarising our findings.

II. STATE OF THE ART: BIVARIATE JUMP-DIFFUSION MODEL

A bivariate jump-diffusion can be modeled via [8, 10]

$$\underbrace{\begin{pmatrix} dy_1(t) \\ dy_2(t) \end{pmatrix}}_{\mathbf{y}} = \underbrace{\begin{pmatrix} N_1 \\ N_2 \end{pmatrix}}_{\mathbf{N}} dt + \underbrace{\begin{pmatrix} g_{1,1} & g_{1,2} \\ g_{2,1} & g_{2,2} \end{pmatrix}}_{\mathbf{g}} \underbrace{\begin{pmatrix} dw_1 \\ dw_2 \end{pmatrix}}_{\mathbf{dw}} + \underbrace{\begin{pmatrix} \xi_{1,1} & \xi_{1,2} \\ \xi_{2,1} & \xi_{2,2} \end{pmatrix}}_{\boldsymbol{\xi}} \underbrace{\begin{pmatrix} dJ_1 \\ dJ_2 \end{pmatrix}}_{\mathbf{dJ}}, \quad (1)$$

Poissonian jumps

* l.rydin.gorjao@fz-juelich.de

† jan.heysel@uni-bonn.de

‡ klaus.lehnertz@ukbonn.de

§ tabar@uni-oldenburg.de

where all the elements of vectors \mathbf{N} , \mathbf{dJ} , and \mathbf{dw} as well as of matrices \mathbf{g} and $\boldsymbol{\xi}$ may, in general, be state- and time-dependent (dependencies not shown for convenience of notation). The drift coefficient is a two-dimensional vector $\mathbf{N} = (N_1, N_2)$ with $\mathbf{N} \in \mathbb{R}^2$, where each dimension of \mathbf{N} , i.e., N_i , may depend on $y_1(t)$ and $y_2(t)$. The diffusion coefficient takes a matrix $\mathbf{g} \in \mathbb{R}^{2 \times 2}$. The two Wiener processes $\mathbf{w} = (w_1, w_2)$ act as independent Brownian noises for the state variables $y_1(t)$ and $y_2(t)$. The diagonal elements of \mathbf{g} comprise the diffusion coefficients of self-contained stochastic diffusive processes, and the off-diagonal elements represent interdependencies between the two Wiener processes, i.e., they result from an interaction between the two processes. Each single-dimensional stochastic process element dw_i of \mathbf{dw} is an increment of a Wiener process, with $\langle dw_i \rangle = 0$, $\langle dw_i^2 \rangle = dt$, $\forall i$.

The discontinuous jump terms are contained in $\boldsymbol{\xi} \in \mathbb{R}^{2 \times 2}$ and $\mathbf{dJ} \in \mathbb{R}^2$, where \mathbf{dJ} represents a two-dimensional Poisson process. These are Poisson-distributed jumps with an average jump rate $\boldsymbol{\lambda} \in \mathbb{R}^2$ in unit time t . The average expected number of jumps of each J_i jump process in a timespan t is $\lambda_i t$.

The jump amplitudes $\boldsymbol{\xi}$ represent a Gaussian-distributed process of mean zero and standard deviation $\xi_{i,j}$, i.e., each $\xi_{i,j}$ is an independent Gaussian distributed valued, with mean zero and standard deviation $\xi_{i,j}$.

In this article merely autonomous system will be considered. Non-ergodic problems are beyond the scope of this work, and a more delicate approach to both bivariate stochastic processes would be needed.

III. BIVARIATE DIFFUSION PROCESSES

Let us begin with two-dimensional diffusion processes, for which the model takes the form

$$\underbrace{\begin{pmatrix} dy_1(t) \\ dy_2(t) \end{pmatrix}}_{\mathbf{y}} = \underbrace{\begin{pmatrix} N_1 \\ N_2 \end{pmatrix}}_{\text{drift}} dt + \underbrace{\begin{pmatrix} g_{1,1} & g_{1,2} \\ g_{2,1} & g_{2,2} \end{pmatrix}}_{\text{diffusion}} \underbrace{\begin{pmatrix} dw_1 \\ dw_2 \end{pmatrix}}_{\mathbf{dw}}. \quad (2)$$

The model consists of six parameters, two for the drift elements and four for the diffusion elements. Being in the presence of a bivariate diffusion process, either by being provided with a set of two-dimensional data, or say, two sets of one-dimensional data, or by numerically generating data with (2), can we uncover the aforementioned parameters strictly from data?

Extensive work exists on this matter, cf. Friedrich *et al*, Phys. Rep. [23]), especially covering purely diffusion processes, and we will use these now as a stepping stone to jump-diffusion processes. Understanding the working and contingencies of recovering the parameters of a diffusion process (2) will serve as a gateway to understand how a similar procedure awards equivalent measures for jump-diffusion processes.

We address this question by numerically integrating hand-picked diffusion processes with given values of the drift \mathbf{N} and diffusion \mathbf{g} coefficients and aim at retrieving these values strictly from the generated data. If the actual and retrieve values match, the reconstruction method is effective. An Euler–Mayurama scheme with a time sampling of 10^{-3} over a total of 10^5 time units (i.e., 10^8 data points) is henceforward employed to numerically integrate the different stochastic processes presented in Ref. [10]. An analysis for varying total time of integration is also presented [24].

Before doing so, we need to revisit the mathematical foundation that allows us to recover, strictly from data, the drift \mathbf{N} and diffusion \mathbf{g} coefficients. For such we introduce the Kramers–Moyal coefficients below.

A stochastic process has a probabilistic description given by the master equation [10, 25]. It describes not a specific stochastic processes in itself, but the probabilistic evolution of the process in time. The master equation accepts an expansion in terms, the Kramers–Moyal expansion, that allows for a purely differential description of the process. More importantly, the coefficients of the expansion, known as the Kramers–Moyal coefficients, entail directly a relation to the aforementioned parameters of a stochastic process given by (1). The exact relation will be given below.

There is although an important detail in what regards the Kramers–Moyal coefficients: they are in themselves not constants, but functions on the underlying space, or in other words, a scalar field, and for our purposes here, they can be understood as two-dimensional surfaces.

Lastly, and more familiar, the Fokker–Planck equation is a truncation of the Kramers–Moyal expansion at second order. It is especially relevant given its connection to physical processes and the Pawula theorem [26]. The Pawula theorem ensures that the truncation is not ill-suited for the underlying process, if the fourth-order Kramers–Moyal coefficient approaches zero in the limit $dt \rightarrow 0$. It is now crucial to understand that the theorem holds for a one-dimensional process, and we are not aware of a proof for higher dimensions. This contrasts the common notion that studying only the first two Kramers–Moyal coefficients of two- or higher-dimensional processes is sufficient (see also, Refs. [8, 9, 27] and references therein).

The Kramers–Moyal coefficients $\mathcal{M}^{[\ell, m]}(x_1, x_2) \in \mathbb{R}^2$ of orders (ℓ, m) are defined as:

$$\begin{aligned} \mathcal{M}^{[\ell, m]}(x_1, x_2) = \\ \lim_{\Delta t \rightarrow 0} \frac{1}{\Delta t} \binom{\ell}{m} \int (y_1(t+\Delta t) - y_1(t))^\ell (y_2(t+\Delta t) - y_2(t))^m \cdot \\ P(y_1, y_2; t+\Delta t | y_1, y_2; t) \Big|_{y_1(t)=x_1, y_2(t)=x_2} dy_1 dy_2, \end{aligned}$$

at a certain measure point (x_1, x_2) , and can be obtained from bivariate time-series $(y_1(t), y_2(t))$. Theoretically, Δt should take the limiting case of $\Delta t \rightarrow 0$, but the restriction of any measuring or storing devices—or the nature of the observables themselves—permits only time-sampled

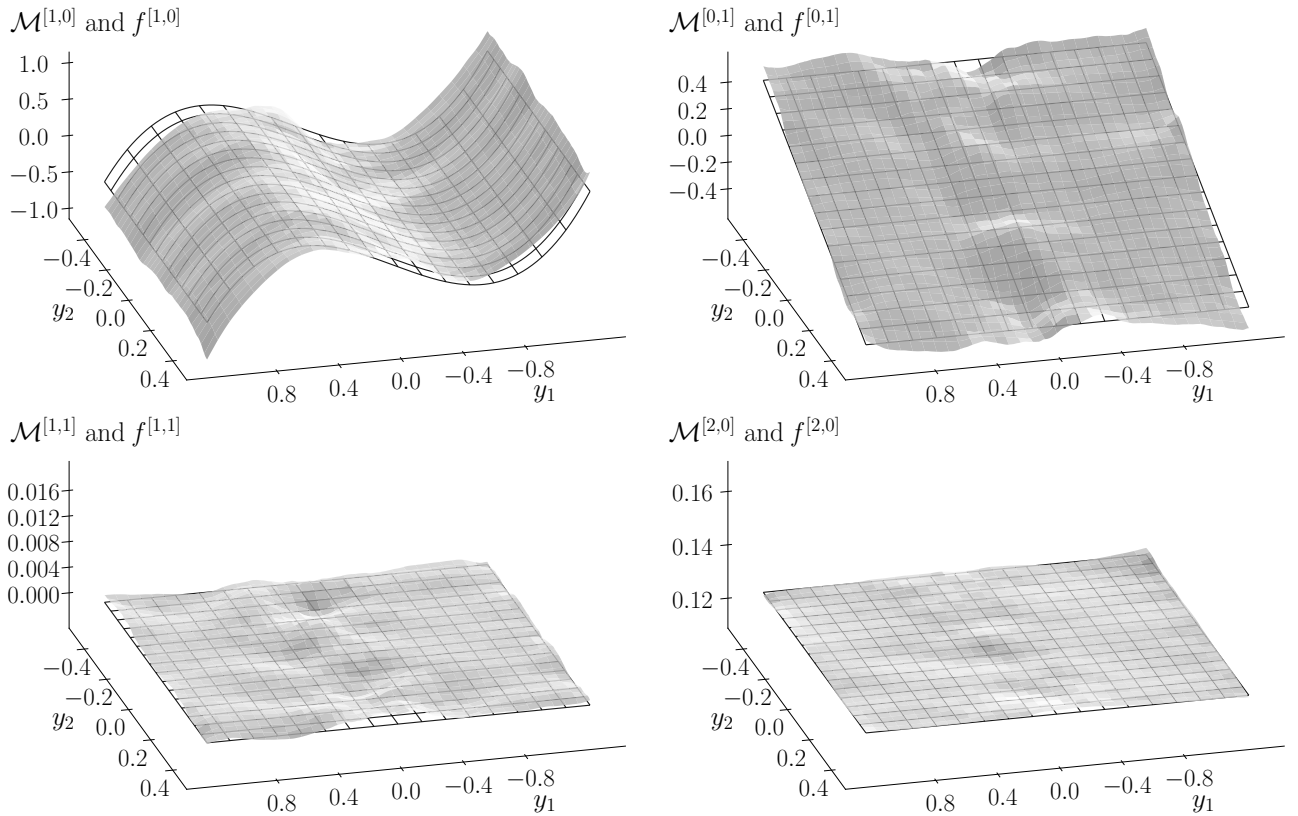


FIG. 1. Two-dimensional Kramers–Moyal coefficients for two independent diffusion processes given by (6). The uncovered Kramers–Moyal surfaces match the expectation, the cubic term in the drift term $N_1 = -x_1^3 + x_1$ along the first variable is visible on the top-left panel, $\mathcal{M}^{[1,0]}$, and the negative negative-slope surface in the top-right panel, $\mathcal{M}^{[0,1]}$. The flat surfaces reproduce as well the expected behaviour of the constant terms involved in the diffusion terms for $\mathcal{M}^{[2,0]}$ on the bottom-left. Moreover, the bottom-right panel $\mathcal{M}^{[1,1]}$, which accounts for the couplings terms of all diffusion terms, is also zero almost everywhere, as expected, given $g_{1,2}$ and $g_{2,1}$ are zero. In each panels the theoretical expected surface is indicate, given by (4) and (5).

or discrete recordings. The relevance and importance of adequate time-sampling was extensively studied and discussed in Ref. [28].

In the limiting case where Δt is equivalent to the sampling rate of the data, the Kramers–Moyal coefficients take the form

$$\mathcal{M}^{[\ell,m]}(x_1, x_2) = \frac{1}{\Delta t} \langle \Delta y_1^\ell \Delta y_2^m |_{y_1(t)=x_1, y_2(t)=x_2}, \quad (3)$$

$$\Delta y_i = y_i(t + \Delta t) - y_i(t).$$

The algebraic relations between the Kramers–Moyal coefficients and functions in (2) are given by [8, 10]

$$\begin{aligned} \mathcal{M}^{[1,0]} &= N_1, \\ \mathcal{M}^{[0,1]} &= N_2, \end{aligned} \quad (4)$$

$$\begin{aligned} \mathcal{M}^{[1,1]} &= g_{1,1}g_{2,1} + g_{1,2}g_{2,2}, \\ \mathcal{M}^{[2,0]} &= \frac{1}{2} [g_{1,1}^2 + g_{1,2}^2], \\ \mathcal{M}^{[0,2]} &= \frac{1}{2} [g_{2,1}^2 + g_{2,2}^2], \end{aligned} \quad (5)$$

where an explicit derivation can be found in Appendix A.

Evidently, this under-determined set of five equations is insufficient to uncover the six parameters of a general stochastic diffusion process. One must bare this in mind, for the same issue will arise again when reconstructing jump-diffusion processes from data, as discussed afterwards. Nonetheless, under certain assumptions, it is possible to reduced the dimension of the problem and therefore obtain a system of equation which is not under-determined. Presented later are criteria for these cases.

To showcase what two-dimensional Kramers–Moyal coefficients are as well as how to identify drift and diffusion terms of bivariate diffusion processes, we present in the following two exemplary processes with *a priori* known coefficients. In this manner, by employing (4) and (5), one can judge the outcome of the Kramers–Moyal coefficient estimation procedure from discrete data in comparison with the expected theoretical functions.

We begin with two uncoupled processes, where one has constant diffusion and a quartic potential as the drift

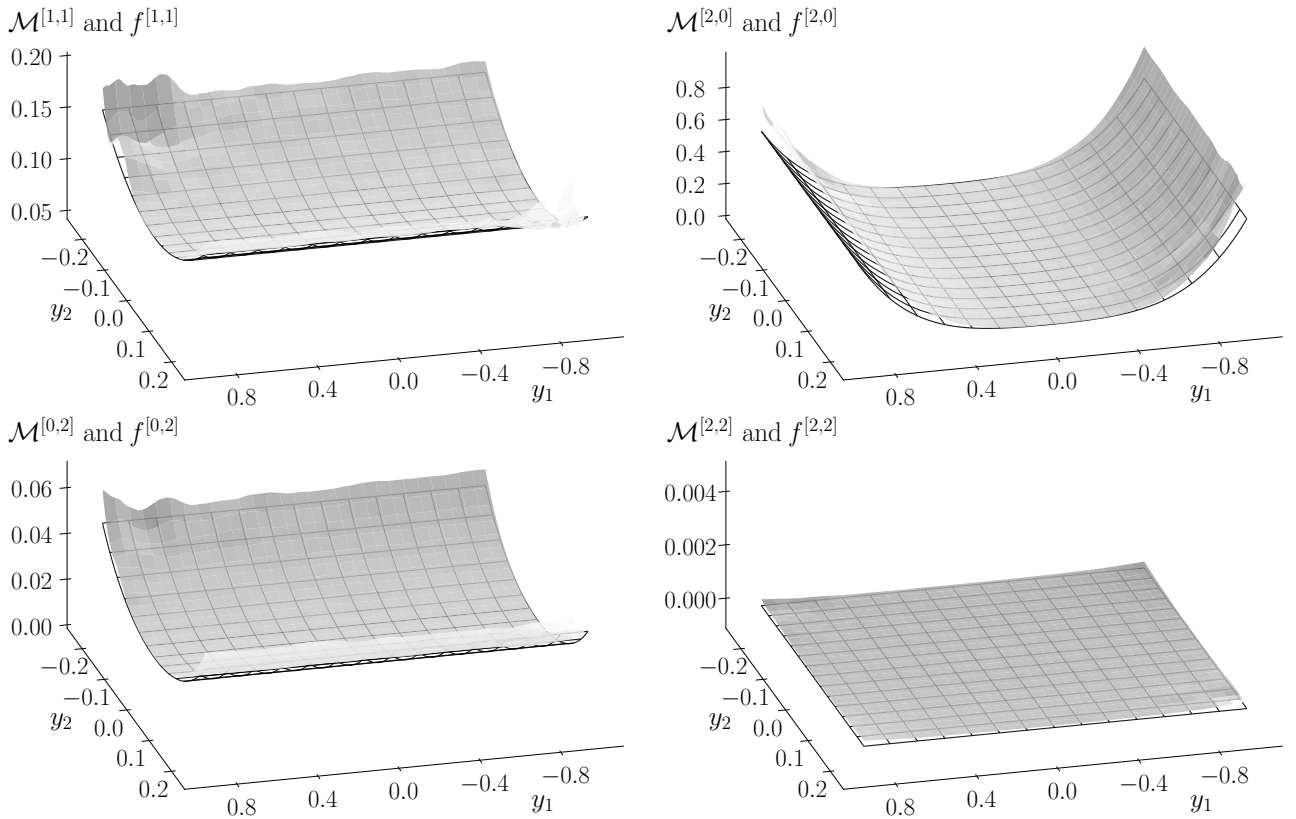


FIG. 2. Two-dimensional Kramers–Moyal coefficients for two independent diffusion processes given by (7) and the theoretical expected functions f associated with each, according to (5). The displayed Kramers–Moyal coefficients $\mathcal{M}^{[1,1]}$, $\mathcal{M}^{[2,0]}$, $\mathcal{M}^{[0,2]}$, and $\mathcal{M}^{[2,2]}$ exhibit the quadratic multiplicative dependencies of the diffusion terms. The Kramers–Moyal coefficient $\mathcal{M}^{[1,1]}$ displays both an offset from zero, as well as a quadratic shape, entailing the desired results emerging from (5), i.e., the noise-coupling term $g_{1,2}$ with $g_{2,2}$. The $\mathcal{M}^{[2,0]}$ Kramers–Moyal coefficient displays an offset, and has a minimum close to $g_{1,1}^2/2 + g_{1,2}^2/2 = 0.13$. Included as well is the higher-order surface $\mathcal{M}^{[2,2]}$ and the theoretically expected value given by (5), i.e., zero. There are no higher-order contributions of the Kramers–Moyal coefficients. All obtained Kramers–Moyal coefficients fit considerably well on their theoretically expected values given by f . The error volumes for the displayed Kramers–Moyal coefficients are: $V_{\text{err}}^{[1,1]} = 0.0289$, $V_{\text{err}}^{[2,0]} = 0.9375$, $V_{\text{err}}^{[0,2]} = 0.0326$, $V_{\text{err}}^{[2,2]} = 0.0001$.

term:

$$\mathbf{N} = \begin{pmatrix} N_1 \\ N_2 \end{pmatrix} = \begin{pmatrix} -x_1^3 + x_1 \\ -x_2 \end{pmatrix}, \quad (6)$$

$$\mathbf{g} = \begin{pmatrix} g_{1,1} & g_{1,2} \\ g_{2,1} & g_{2,2} \end{pmatrix} = \begin{pmatrix} 0.5 & 0.0 \\ 0.0 & 0.5 \end{pmatrix},$$

In Fig. 1, we show the corresponding $\mathcal{M}^{[1,0]}$, $\mathcal{M}^{[0,1]}$, $\mathcal{M}^{[1,1]}$, and $\mathcal{M}^{[2,0]}$ Kramers–Moyal coefficients together with the theoretically expected functions. The per-design cubic-linear function ($N_1 = -x_1^3 + x_1$) acting as drift coefficient along the first dimension as well as the negatively-sloped surface of $N_2 = -x_2$ are evident. Likewise, the constant diffusion term leads to a flat constant-valued $\mathcal{M}^{[2,0]}$ Kramers–Moyal coefficient, and the absence of any non-diagonal elements ($g_{1,2} = g_{2,1} = 0$) agrees with the zero-valued $\mathcal{M}^{[1,1]}$ Kramers–Moyal coefficient.

We next extend (6) by adding multiplicative noise to the diffusion term and by including a noise coupling term

$g_{1,2} \neq 0$:

$$\mathbf{N} = \begin{pmatrix} N_1 \\ N_2 \end{pmatrix} = \begin{pmatrix} -x_1^3 + x_1 \\ -x_2 \end{pmatrix}, \quad (7)$$

$$\mathbf{g} = \begin{pmatrix} g_{1,1} & g_{1,2} \\ g_{2,1} & g_{2,2} \end{pmatrix} = \begin{pmatrix} 0.1 + x_1^2 & 0.5 \\ 0.0 & 0.2 + 2x_2^2 \end{pmatrix}.$$

The recovered Kramers–Moyal coefficients of the drift terms remains unaltered, but as posited, the second-order Kramers–Moyal coefficients, i.e., $\mathcal{M}^{[1,1]}$, $\mathcal{M}^{[2,0]}$, $\mathcal{M}^{[0,2]}$, and $\mathcal{M}^{[2,2]}$, exhibit the impact of the multiplicative noise. In Fig. 2, the $\mathcal{M}^{[1,1]}$, $\mathcal{M}^{[2,0]}$, and $\mathcal{M}^{[0,2]}$ Kramers–Moyal coefficients are displayed. The quadratic multiplicative dependencies of $\mathcal{M}^{[2,0]}$, and $\mathcal{M}^{[0,2]}$, and their offset from zero, is evident, but more pertinently, one can notice $\mathcal{M}^{[1,1]}$ displays the expected shape arising from (5), i.e., this value is non-zero and exhibits the parabolic shape of $g_{1,2} \cdot g_{2,2} = 0.5(0.2 + 2x_2^2)$. For $x_2 = 0$, i.e., the minimum, the obtained value coincides with 0.1, as expected.

Alongside in Fig. 2 are displayed the theoretically ex-

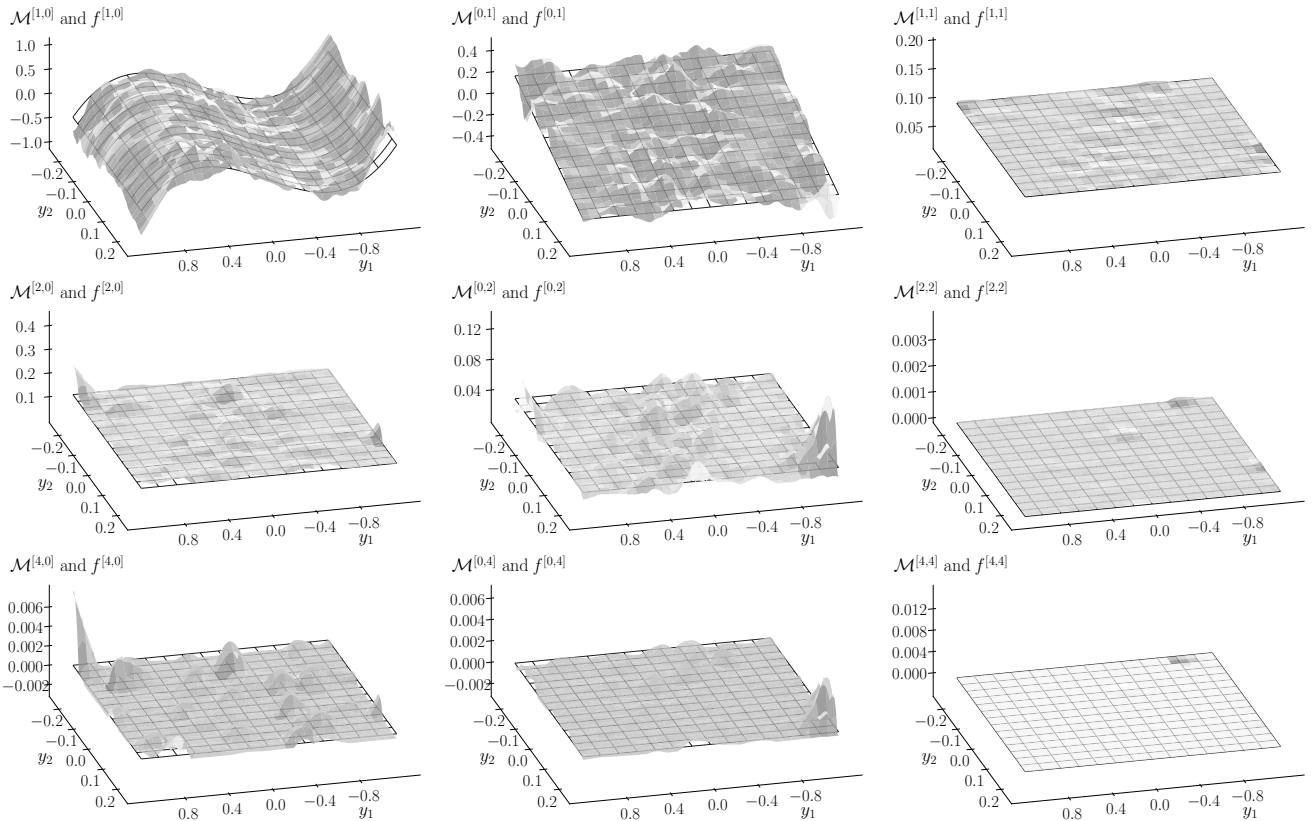


FIG. 3. Two-dimensional Kramers–Moyal coefficients of bivariate diffusion processes given by (15), with $\phi = 0.0$, together with the theoretically expected functions f associated with each Kramers–Moyal coefficient according to (10), (11), and (12). The Kramers–Moyal coefficients $\mathcal{M}^{[1,0]}$, $\mathcal{M}^{[0,1]}$, $\mathcal{M}^{[1,1]}$, $\mathcal{M}^{[2,0]}$, $\mathcal{M}^{[0,2]}$, $\mathcal{M}^{[2,2]}$, $\mathcal{M}^{[4,0]}$, $\mathcal{M}^{[0,4]}$, and $\mathcal{M}^{[4,4]}$ are shown. Although seemingly small, the higher order moments are all present and non-zero. Both $\mathcal{M}^{[4,0]}$ and $\mathcal{M}^{[0,4]}$ have values approximate to 0.012 and 0.009, as (12) dictates. All obtained surfaces fit with their respective theoretical expected values given by f . The error volume for the displayed Kramers–Moyal coefficients are: $V_{\text{err}}^{[1,0]} = 0.6774$, $V_{\text{err}}^{[0,1]} = 0.1836$, $V_{\text{err}}^{[1,1]} = 0.0008$, $V_{\text{err}}^{[2,0]} = 0.0147$, $V_{\text{err}}^{[0,2]} = 0.0117$, $V_{\text{err}}^{[2,2]} = 0.0001$, $V_{\text{err}}^{[4,0]} = 0.0147$, $V_{\text{err}}^{[0,4]} = 0.0051$, $V_{\text{err}}^{[4,4]} < 0.0001$.

pected Kramers–Moyal coefficients f , given by (4) and (5). These serve to evaluate the quality of the non-parametrically estimated Kramers–Moyal coefficients in comparison to the actual theoretically expected results.

In order to relate the results obtained from studying the Kramers–Moyal coefficients against the theoretical functions, we now propose a method to assess the difference between the values of the theoretically expected functions and the estimated values of the Kramers–Moyal coefficients. Since for bivariate processes the Kramers–Moyal coefficients are two dimensional—as are the parameters of (1)—an adequate distance measure between the resulting two-dimensional *surfaces* is required.

Following Ref. [29], we propose a distance measure that allows for the variability of the density of data in some regions of the underlying space. Let $f(y_1, y_2)$ denote the theoretical value introduced in the model, i.e., a non-linear combination of the various parameters of the system. The distance between each surface at the same point

in space can be defined as

$$\iint_U \left(\mathcal{M}^{[n,m]}(y_1, y_2) - f^{[n,m]}(y_1, y_2) \right)^2 dy_1 dy_2 = V^2, \quad (8)$$

where U denotes the domain of $\mathcal{M}^{[n,m]}(y_1, y_2)$. The least-squared distance volume V between the surfaces is zero if $\mathcal{M}^{[n,m]}(y_1, y_2) = f^{[n,m]}(y_1, y_2)$. It is this volume that one aims to minimise such that the reconstructed Kramers–Moyal coefficients match the underlying theoretical functions in the model. Since $\mathcal{M}^{[n,m]}(y_1, y_2)$ is a real-valued function measured over a distribution space U , the density of data points is not uniform over U . This implies that a comparative measure on distances between $\mathcal{M}^{[n,m]}(y_1, y_2)$ and $f^{[n,m]}(y_1, y_2)$ would be non-normalised to the density of points of the space. We therefore introduce a normalisation to (8) that ensures the less dense areas of U are normalised accordingly, thus mitigating the effect of scarcity of points at the borders of U and an overestimation of V due to outliers in the distribution. We derive such a normalisation by considering the zeroth-order Kramers–Moyal coeffi-

cient $\mathcal{M}^{[0,0]}(y_1, y_2)$ which captures exactly the density of points in U , although it is in itself not normalised as a distribution. The resulting normalised volume error measure V_{err} between surfaces takes the form (state dependencies not explicit)

$$\iint_U \frac{\mathcal{M}^{[0,0]}}{|\mathcal{M}^{[0,0]}|} \left(\mathcal{M}^{[n,m]} - f^{[n,m]} \right)^2 dy_1 dy_2 = V_{\text{err}}^2, \quad (9)$$

where $|\cdot|$ denotes the normalisation of the distribution, i.e.,

$$|\mathcal{M}^{[0,0]}| = \iint_U \mathcal{M}^{[0,0]} dy_1 dy_2.$$

With this at hand, it is now possible to relate theoretical and numerical results and to quantify the deviation of the obtained Kramers–Moyal coefficients from the functions employed.

In Fig. 1 and Fig. 2 the error volume measurement V_{err} was already indicated. It is important to notice that by itself, the error volume estimation carries no meaning, but in a comparative sense, it allows one to understand which estimations are closer to the theoretical values, as will be presented later. Naturally, values close to zero indicate a very good matching between estimation and actual values.

IV. BIVARIATE JUMP-DIFFUSION PROCESSES

The Kramers–Moyal coefficients of bivariate jump-diffusion processes take the following form (under the parameter prescription used in the jump-diffusion model

in Eq. (1)) [8–10]

$$\begin{aligned} \mathcal{M}^{[1,0]} &= N_1 \\ \mathcal{M}^{[0,1]} &= N_2 \end{aligned} \quad (10)$$

$$\begin{aligned} \mathcal{M}^{[1,1]} &= g_{1,1}g_{2,1} + g_{1,2}g_{2,2} \\ \mathcal{M}^{[2,0]} &= \frac{1}{2} [g_{1,1}^2 + s_{1,1}\lambda_1 + g_{1,2}^2 + s_{1,2}\lambda_2] \\ \mathcal{M}^{[0,2]} &= \frac{1}{2} [g_{2,1}^2 + s_{2,1}\lambda_1 + g_{2,2}^2 + s_{2,2}\lambda_2] \\ \mathcal{M}^{[2,2]} &= s_{1,1}s_{2,1}\lambda_1 + s_{1,2}s_{2,2}\lambda_2 \end{aligned} \quad (11)$$

$$\begin{aligned} \mathcal{M}^{[4,0]} &= \frac{3}{24} [s_{1,1}^2\lambda_1 + s_{1,2}^2\lambda_2] \\ \mathcal{M}^{[0,4]} &= \frac{3}{24} [s_{2,1}^2\lambda_1 + s_{2,2}^2\lambda_2] \\ \mathcal{M}^{[4,4]} &= 9 [s_{1,1}^2s_{2,1}^2\lambda_1 + s_{1,2}^2s_{2,2}^2\lambda_2] \end{aligned} \quad (12)$$

$$\begin{aligned} \mathcal{M}^{[6,0]} &= \frac{15}{6!} [s_{1,1}^3\lambda_1 + s_{1,2}^3\lambda_2] \\ \mathcal{M}^{[0,6]} &= \frac{15}{6!} [s_{2,1}^3\lambda_1 + s_{2,2}^3\lambda_2] \\ \mathcal{M}^{[6,6]} &= 225 [s_{1,1}^3s_{2,1}^3\lambda_1 + s_{1,2}^3s_{2,2}^3\lambda_2] \end{aligned} \quad (13)$$

$$\begin{aligned} \mathcal{M}^{[8,0]} &= \frac{105}{8!} [s_{1,1}^4\lambda_1 + s_{1,2}^4\lambda_2] \\ \mathcal{M}^{[0,8]} &= \frac{105}{8!} [s_{2,1}^4\lambda_1 + s_{2,2}^4\lambda_2] \end{aligned} \quad (14)$$

where $\langle \xi_{ij}^{2\ell} \rangle = \sigma_{\xi_{ij}}^{2\ell} = s_{ij}^\ell$ are the variances of the Gaussian-distributed jump amplitudes. An extended derivation can be found in App. A. The last equations here are taken from the general form

$$M^{[\ell,m]} = \binom{\ell}{m} \frac{(2\ell)! (2m)!}{2^\ell \ell! 2^m m!} [\langle \xi^\ell \rangle \langle \xi^m \rangle \lambda_1 + \langle \xi^\ell \rangle \langle \xi^m \rangle \lambda_2].$$

A. Understanding the impact of the jumps

As an illustrative case-study, we investigate a general jump-diffusion process that is based on (7), but excluding the multiplicative diffusion terms. To take into account the effect of the jump terms, but maintaining the system independent in at least one of the dimensions, we extend (7) to include jumps only in the diagonal terms of ξ

$$\begin{aligned} \mathbf{N} &= \begin{pmatrix} N_1 \\ N_2 \end{pmatrix} = \begin{pmatrix} -x_1^3 + x_1 \\ -x_2 \end{pmatrix} \\ \mathbf{g} &= \begin{pmatrix} g_{1,1} & g_{1,2} \\ g_{2,1} & g_{2,2} \end{pmatrix} = \begin{pmatrix} 0.1 & 0.5 \\ 0.0 & 0.2 \end{pmatrix} \\ \xi &= \begin{pmatrix} \xi_{1,1} & \xi_{1,2} \\ \xi_{2,1} & \xi_{2,2} \end{pmatrix} = \begin{pmatrix} 0.2 & 0.0 \\ \phi & 0.1 \end{pmatrix} \\ \lambda &= \begin{pmatrix} \lambda_1 \\ \lambda_2 \end{pmatrix} = \begin{pmatrix} 0.1 \\ 0.3 \end{pmatrix}, \end{aligned} \quad (15)$$

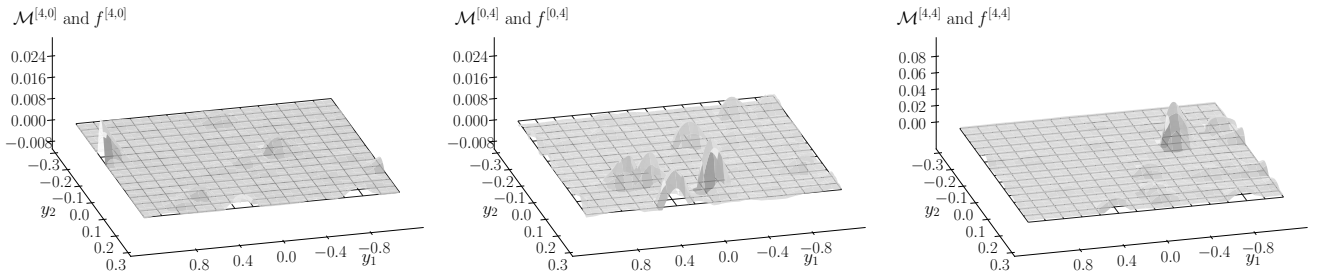


FIG. 4. Two-dimensional $\mathcal{M}^{[4,0]}$, $\mathcal{M}^{[0,4]}$, and $\mathcal{M}^{[4,4]}$ Kramers–Moyal coefficients of a bivariate jump-diffusion processes given by (15), with $\phi = 0.3$, and all theoretical expected functions f associated with each Kramers–Moyal coefficient, according to (10), (11), and (12). Notice the estimation of the Kramers–Moyal coefficients agree well with the theoretical expected functions f in all orders. For further details, see App. B.

where for the present case, $\phi = 0.0$. In this manner, jumps are added to the first dimension of the process, having an amplitude of $\xi_{1,1} = 0.2$ and occurring every $0.1t$, given $\lambda_1 = 0.1$. Similarly, to the second dimension, $\xi_{2,2} = 0.1$, but the jumps occur three times more often than the aforementioned, given $\lambda_2 = 0.3$. We note that the parameters taken here carry no physical meaning, at least to the extent of what is known.

In Fig. 3 the effects of having jumps can be seen across all Kramers–Moyal coefficients. The previously smooth surfaces become rugged from the fast variations emerging due to the jumps, and the higher-order Kramers–Moyal coefficients deviate from zero. Although they remain small, in comparison to the other coefficients, they no longer amount to zero. This indicates that the lower-order modelling, as the white-noise Langevin equations, and the common assumption stemming from the Pawula theorem are invalid for this process. Modelling these stochastic process taking only into account the first two orders of the Kramers–Moyal expansion of the master equation describing the process is therefore incorrect. Higher-order Kramers–Moyal are non-negligible, and as mentioned above, there is strong indication of the presence of these higher-order effects in data, implying directly the necessity of the modelling of stochastic process with higher-order models, such as the jump-diffusion process.

In order to understand further if it is possible to uncover the jump amplitude terms of coupled processes, one can use the previous model (15), with $\phi = 0.3$, effectively introducing a coupling in the off-diagonal jump matrix ξ , and thus coupling the jump process of one of the dimensions to the other.

In Fig 4, the fourth-order Kramers–Moyal coefficients are presented. Here it is especially relevant to look at the higher-order Kramers–Moyal coefficients, to better understand the impact of the jumps. As can be seen, the fact that $\phi = 0.3$, i.e., that there exists a coupling of the Poisson jump processes of the two dimensions of the system. The effect of this coupling is visible, although small, in the $\mathcal{M}^{[4,4]}$ Kramers–Moyal coefficient, which is no longer zero. Likewise are the $\mathcal{M}^{[4,0]}$ and $\mathcal{M}^{[0,4]}$ Kramers–Moyal coefficients also non-zero.

All Kramers–Moyal coefficients up to the eight order, for the same model (15), with $\phi = 0.3$, presented in Fig 4, are found in the App. B.

B. Criteria for recovering parameters in diffusion and jump-diffusion model

Interestingly, for the case of vanishing off-diagonal elements $g_{2,1}$ and $\xi_{1,2}$, we can identify ways to recover the remaining parameters of the system.

First, given the noise $d\omega$ in these system is Gaussian distributed, \mathbf{g} is sign-reversal symmetric, thus one can consider it takes only positive values. One obtains that, if $\mathcal{M}^{[1,1]} = 0$ then at least two elements of \mathbf{g} must be zero, and if $\mathcal{M}^{[2,2]} = 0$ then at least two elements of ξ must be zero.

These findings reduce the dimensionality of the parameter estimation and ensure that the underlying processes are invariantly less complex than the full-fledged description of (1), although they do not grant which parameters are zero valued.

Second, if one either employs a heuristic argument of independence of the jump processes or neglects the off-diagonal jump amplitudes $\xi_{1,2}$ and $\xi_{2,1}$ (e.g. by assuming they are small compared to the diagonal terms of ξ), one finds the following approximations:

$$\begin{aligned} \frac{1}{5} \frac{\mathcal{M}^{[6,0]}}{\mathcal{M}^{[4,0]}} &= \frac{1}{5} \frac{15}{3} \frac{s_{1,1}^3 \lambda_1}{s_{1,1}^2 \lambda_1} = s_{1,1}, \\ \frac{1}{5} \frac{\mathcal{M}^{[0,6]}}{\mathcal{M}^{[0,4]}} &= \frac{1}{5} \frac{15}{3} \frac{s_{2,2}^3 \lambda_2}{s_{2,2}^2 \lambda_2} = s_{2,2}. \end{aligned} \quad (16)$$

Likewise, the jump rates λ_1 and λ_2 can be obtained equivalently as

$$\begin{aligned} \frac{105}{9} \frac{\mathcal{M}^{[4,0]^2}}{\mathcal{M}^{[8,0]}} &= \frac{105}{9} \frac{3^2}{105} \frac{(s_{1,1}^2 \lambda_1)^2}{s_{1,1}^4 \lambda_1} = \lambda_1, \\ \frac{105}{9} \frac{\mathcal{M}^{[0,4]^2}}{\mathcal{M}^{[0,8]}} &= \frac{105}{9} \frac{3^2}{105} \frac{(s_{2,2}^2 \lambda_2)^2}{s_{2,2}^4 \lambda_2} = \lambda_2. \end{aligned} \quad (17)$$

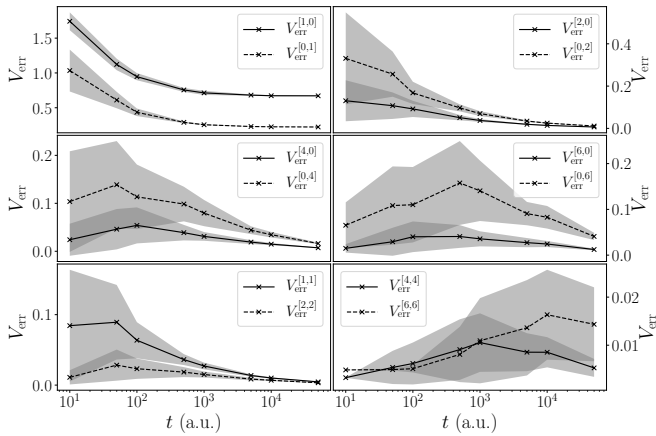


FIG. 5. [Abscissa in logarithmic scale] Error volume V_{err} for a bivariate jump-diffusion process (15) integrated for increasing number of total points. The time t , in arbitrary units, indicates the number of points for a time series numerically integrated with a time-sampling of 10^{-3} , that is, $t = 10$ is a two-dimensional data series with 2×10^4 points. Each process is numerically integrated with random initial conditions 50 times, and the average value of V_{err} and one-standard deviations (shaded) are displayed. Notice the clear decrease on all non-mixed Kramers–Moyal, e.g. $\mathcal{M}^{[2,0]}$ or $\mathcal{M}^{[0,2]}$. The mixed Kramers–Moyal, like $\mathcal{M}^{[4,4]}$ or $\mathcal{M}^{[6,6]}$ can present themselves as non-decreasing, but are overall considerable smaller in value. Compare to Fig. 6.

Taking the model (15) discussed previously, with $\phi = 0.0$, and following (16), we obtain

$$\begin{aligned} s_{1,1}^{\text{est}} &= 0.1642 \approx 0.2 = s_{1,1}^{\text{real}}, \\ s_{2,2}^{\text{est}} &= 0.0942 \approx 0.1 = s_{2,2}^{\text{real}}. \end{aligned}$$

This values are just shy of the correct value, even for such simplistic measure. Although not perfect measures, they serve as stepping stones in obtaining a deeper understanding of the process being analysed.

The criteria and approximations are especially relevant when constructing or analysing systems which are known to have a specific unidirectional coupling form, e.g. master-slave system, where for example the noise or the slave system are dictated by the driving master system.

C. Influencing parameters

In order to validate the quality of the non-parametric recovery of the Kramers–Moyal coefficients, we turn to two critical points: firstly, bivariate processes may require a high number of data points in a data series for the estimation to be reliable. Secondly, the interplay between the drift, diffusion and jump parts of a stochastic process may render the estimation incorrect.

To this purposes, we include a more contrived model involving couplings and interactions in both the diffusion

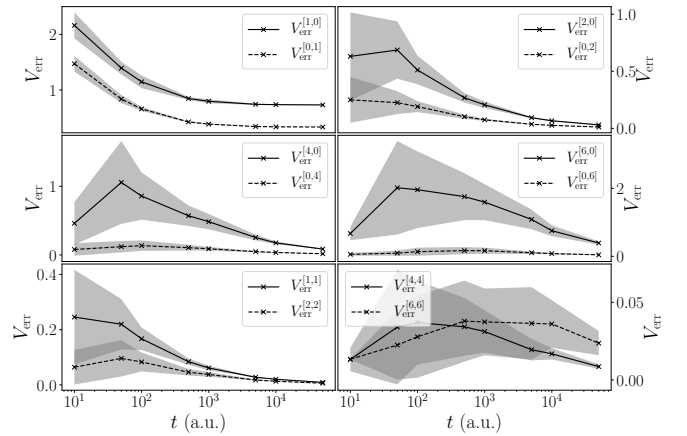


FIG. 6. [Abscissa in logarithmic scale] Error volume V_{err} for the bivariate jump-diffusion process (18), with $\alpha = \beta = 0.3$, integrated for increasing number of total points. The time t , in arbitrary units, indicates the number of points. See Fig. 5 for details. The average value of V_{err} and one-standard deviations (shaded) are displayed. Again evidenced is the decrease on all non-mixed Kramers–Moyal. The mixed-terms do not seem to decrease with the increasing density of data points, but are small in error volume. Compare to Fig. 5.

and jump terms, thus theoretically resulting in having all higher-order Kramers–Moyal coefficients non-zero, and especially the mixed Kramers–Moyal coefficients. The parameters read

$$\begin{aligned} \mathbf{N} &= \begin{pmatrix} N_1 \\ N_2 \end{pmatrix} = \begin{pmatrix} -x_1^3 + x_1 \\ -x_2 \end{pmatrix}, \\ \mathbf{g} &= \begin{pmatrix} g_{1,1} & g_{1,2} \\ g_{2,1} & g_{2,2} \end{pmatrix} = \begin{pmatrix} 0.1 & 0.5 \\ \alpha & 0.2 \end{pmatrix}, \\ \boldsymbol{\xi} &= \begin{pmatrix} \xi_{1,1} & \xi_{1,2} \\ \xi_{2,1} & \xi_{2,2} \end{pmatrix} = \begin{pmatrix} 0.2 & 0.5 \\ \beta & 0.1 \end{pmatrix}, \\ \boldsymbol{\lambda} &= \begin{pmatrix} \lambda_1 \\ \lambda_2 \end{pmatrix} = \begin{pmatrix} 0.1 \\ 0.3 \end{pmatrix}, \end{aligned} \quad (18)$$

where the diffusion parameter α and the jump parameter β can be freely varied.

Let us focus firstly on the number of data points in a time series.

Utilising models (15) and (18), with $\alpha = \beta = 0.3$, and numerically integrating the results for a set of different number of points allows one to study the effects of the scarcity of the number of points in a dataset in direct contrast to the ability of estimating the Kramers–Moyal coefficients. By again employing the error volume measure V_{err} one can evaluate comparatively the different error volumes for each Kramers–Moyal coefficients.

In Fig. 5 and Fig. 6, for models (15) and (18), respectively, are exhibited the error volume V_{err} for the Kramers–Moyal coefficients for increasing number of data points. The reliability of the recovery of parameters is validated for higher amount of data, as expected, although the scarcity of data posits no extensive problem for the

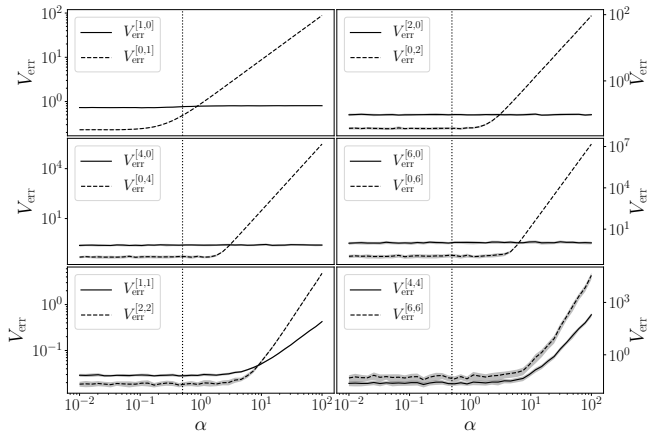


FIG. 7. [Double logarithmic scale] Error volume V_{err} for the bivariate jump-diffusion process (18) for a varying noise term α in $[10^{-2}, 10^2]$. The vertical dotted line indicates the biggest diffusion term value, in this case $g_{1,2} = 0.5$ to serve as a guide to compare to the value of α . A small value of the noise term α , in comparison to the remaining diffusion terms, ensures a good reconstruction, i.e., a small error volume V_{err} . The average and one-standard deviations (shaded) are displayed. For each point 50 iterations are taken, each with a total integration time of 5×10^3 and a time sampling of 10^{-3} , totaling thus 5×10^6 points. Statistical outliers are discarded.

calculation. It is especially important to notice that a smaller time series entails naturally fewer jumps in the process, hindering the possibility of accurately recovering the jump terms from short data series. From values of $t = 10^3$, i.e., 10^6 data points, the estimation seems reliable, the standard deviations become minute, and most error values approach zero, i.e., the theoretical and estimated Kramers–Moyal surfaces are close.

One remark is necessary on the recover of the drift terms. The presence of noise and jumps of the system takes its toll on the recovery of the exact form of the Kramers–Moyal coefficients, as well as the explicit dependence of the state variables, i.e., the quartic potential in both (15) and (18). A finer time sampling can help improve the results.

To further test the limitation of retrieving the Kramers–Moyal coefficients from data, model (18) is utilised once more, but now one permits the free parameters to vary, allowing the study the effects of increasing the noise term α and the jump term β .

For each variation of the parameters separately, Fig. 7 and Fig. 8 exhibit effect of increasing the parameters on the recovery of the Kramers–Moyal coefficients. In Fig. 7, the diffusion term α is varied from $[10^{-2}, 10^2]$, with $\beta = 0.3$. A considerable impact on the error volume V_{err} takes place after the order of magnitude on the diffusion parameter α is ten-fold bigger in comparison to the other diffusion parameters. Similarly, in Fig. 8 the jump term β varies within $[10^{-2}, 10^2]$, whilst $\alpha = 0.3$ remains fixed. The increasing value of the jump term β drive the error volume V_{err} already when its value is of similar size

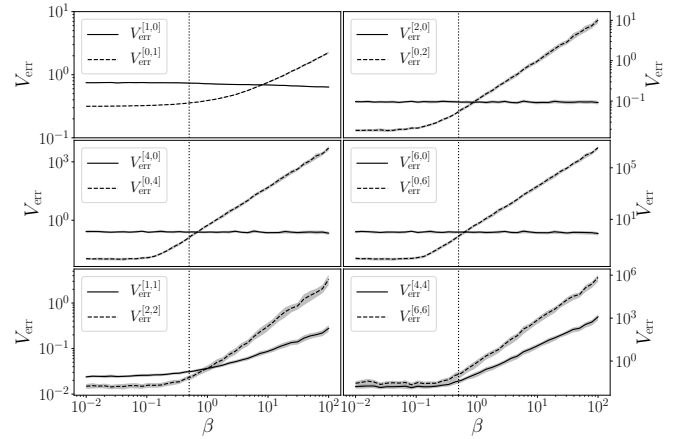


FIG. 8. [Double logarithmic scale] Error volume V_{err} for the bivariate jump-diffusion process (18) for a varying jump term β in $[10^{-2}, 10^2]$. The vertical dotted line indicates the biggest jump term value $\xi_{1,2} = 0.5$ to compare with β . As in direct analogy to Fig. 7, a small jump term β ensures a good reconstruction, i.e., a small error volume for V_{err} . Growing values of the jump term β in comparison to the other parameters in the system make the reconstruction unreliable. The average and one-standard deviations (shaded) are displayed. For each point 50 iterations are taken, each with a total integration time of 5×10^3 and a time sampling of 10^{-3} , totaling thus 5×10^6 points. Statistical outliers are discarded.

to the remaining parameters.

Rounding up, this reveals the difficulty of recovering the Kramers–Moyal coefficients, ergo the parameters of the system, in the presence of jumps in the system. Nonetheless, the results for modelled data indicate that the current understanding, modelling, and numerical recovery of the Kramers–Moyal surfaces, for the case of jumps of comparable size to the diffusion terms, is possible and reliable.

This being the case, it is a further indication that outdated lower-order analyses of data, especially under the assumption that the higher-order moments vanish, may be more damaging than beneficial to the understanding of the nature on the processes generating the data under examination. Adopting higher-order models, as the jump-diffusion model, now that both the mathematical understanding of the process is clear and that the estimations are reliable, may prove to be very beneficial when working with data riddled with jumps.

V. CONCLUSION

The bivariate jump-diffusion model presented, yielding extensive mathematical implications and application, is a novel model embodying the necessary parameters to describe any coupled system of jumpy and diffusive characteristics.

With a view to field data analyses, we note that our approach can easily be extended to non-stationary

time series, e.g., by employing averaging techniques [30]. A kernel-based estimation technique [8, 31] was applied for calculating the Kramers–Moyal coefficients, but more traditional—yet less robust—histogram methods are equivalently applicable. Our novel approach to distinguish diffusive from jumpy stochastic behaviour in time series, thus provides a general avenue to better understand the dynamics of coupled complex systems.

ACKNOWLEDGEMENTS

The authors would like to thank Thorsten Rings and Mehrnaz Anvari for interesting discussions. L. R. G. thanks Francisco Meirinhos for the tremendous help in devising the methodology behind the results. L.R.G. thanks Dirk Witthaut for everlasting support, and gratefully acknowledges support by the Helmholtz Association, via the joint initiative *Energy System 2050 - A Contribution of the Research Field Energy* and the grant No. VH-NG-1025.

-
- [1] M. B. Weissman, “ $\frac{1}{f}$ noise and other slow, nonexponential kinetics in condensed matter,” *Rev. Mod. Phys.* **60**, 537–571 (1988).
- [2] Gurdip Bakshi, Charles Cao, and Zhiwu Chen, “Empirical performance of alternative option pricing models,” *Journal of Finance* **52**, 2003–2049 (1997).
- [3] Darrell Duffie, Jun Pan, and Kenneth Singleton, “Transform analysis and asset pricing for affine jump-diffusions,” *Econometrica* **68**, 1343–1376 (2000).
- [4] Torben G Andersen, Luca Benzoni, and Jesper Lund, “An empirical investigation of continuous-time equity return models,” *Journal of Finance* **57**, 1239–1284 (2002).
- [5] Sanjiv R Das, “The surprise element: jumps in interest rates,” *J. Econometrics* **106**, 27–65 (2002).
- [6] Michael Johannes, “The statistical and economic role of jumps in continuous-time interest rate models,” *J. Finance* **59**, 227–260 (2004).
- [7] Z. Cai and Y. Hong, “Some recent developments in nonparametric finance,” in *Nonparametric Econometric Methods*, Advances in Econometrics, Volume 25, edited by Q. Li and J. S. Racine (Emerald Group Publishing Limited, 2009) pp. 379–432.
- [8] Mehrnaz Anvari, M Reza Rahimi Tabar, Joachim Peinke, and Klaus Lehnertz, “Disentangling the stochastic behavior of complex time series,” *Sci. Rep.* **6**, 35435 (2016).
- [9] Klaus Lehnertz, Lina Zabawa, and M Reza Rahimi Tabar, “Characterizing abrupt transitions in stochastic dynamics,” *New J. Physics* **20**, 113043 (2018).
- [10] M. Reza Rahimi Tabar, *Analysis and Data-Based Reconstruction of Complex Nonlinear Dynamical Systems: Using the Methods of Stochastic Processes* (Springer-Nature, 2019).
- [11] see, e.g., R. T. Wakai and D. J. V. Harlingen, *Appl. Phys. Lett.* **49**, 593 (1986); C. T. Rogers, R. A. Buhrman, H. Kroger, and L. N. Smith, *Appl. Phys. Lett.* **49**, 1107 (1986); M. Matsuda and S. Kuriki, *Appl. Phys. Lett.* **53**, 621 (1988); K. S. Ralls and R. A. Buhrman, *Phys. Rev. Lett.* **60**, 2434 (1988); D. H. Cobden, A. Savchenko, M. Pepper, N. K. Patel, *Rev. Lett.* **69**, 502 (1992); I. Bloom, A. C. Marley, and M. B. Weissman, *Phys. Rev. Lett.* **71**, 4385 (1993); P. D. Dresselhaus, L. Ji, S. Han, J. E. Lukens, and K. K. Likharev, *Phys. Rev. Lett.* **72**, 3226 (1994); M. J. Ferrari, M. Johnson, F. C. Wellstood, J. J. Kingston, T. J. Shaw, and J. Clarke, *J. Low Temp. Phys.* **94**, 15 (1994); R. J. P. Keijsers, O. I. Shklyarevskii, and H. van Kempen, *Phys. Rev. Lett.* **77**, 3411 (1996); A. L. Efros and M. Rosen, *Phys. Rev. Lett.* **78**, 1110 (1997); E. Shung, T. F. Rosenbaum, S. N. Coppersmith, G. W. Crabtree, and W. Kwok, *Phys. Rev. B* **56**, R11431, (1997).
- [12] Luca Gammaitoni, Peter Hänggi, Peter Jung, and Fabio Marchesoni, “Stochastic resonance,” *Rev. Mod. Phys.* **70**, 223–287 (1998).
- [13] D. Brockmann and L. Hufnagel, “Front propagation in reaction-superdiffusion dynamics: Taming lévy flights with fluctuations,” *Phys. Rev. Lett.* **98**, 178301 (2007).
- [14] Simon Vaughan, “Random time series in astronomy,” *Phil. Trans. Roy. Soc. London A: Mathematical, Physical and Engineering Sciences* **371**, 20110549 (2013).
- [15] M Anvari, G Lohmann, M Wächter, P Milan, E Lorenz, D Heinemann, M Reza Rahimi Tabar, and Joachim Peinke, “Short term fluctuations of wind and solar power systems,” *New J. Physics* **18**, 063027 (2016).
- [16] T. M. Lenton, *Nat. Clim. Change* **1**, 201 (2011); M. Scheffer, S. R. Carpenter, T. M. Lenton, J. Bascompte, W. Brock, V. Dakos, J. van de Koppel, I. A. van de Leemput, S. A. Levin, E. H. van Nes, M. Pascual, and J. Vandermeer, *Science* **338**, 344 (2012).
- [17] Yacine Ait-Sahalia, “Telling from discrete data whether the underlying continuous-time model is a diffusion,” *J. Finance* **57**, 2075–2112 (2002).
- [18] Suzanne S. Lee and Per A. Mykland, “Jumps in financial markets: A new nonparametric test and jump dynamics,” *Rev. Financial Stud.* **21**, 2535–2563 (2008).
- [19] Bedartha Goswami, Niklas Boers, Aljoscha Rheinwalt, Norbert Marwan, Jobst Heitzig, Sebastian FM Breitenbach, and Jürgen Kurths, “Abrupt transitions in time series with uncertainties,” *Nat. Commun.* **9**, 48 (2018).
- [20] D. Colquhoun and A. Hawkes, *Proc. R. Soc. Lond. B* **211**, 205 (1981); L. S. Liebovitch, *Ann. Biomed. Eng.* **16**, 483 (1988).
- [21] S. Martinez-Conde, S. L. Macknik, and D. H. Hubel, *Nat. Rev. Neurosci.* **5**, 229 (2004); H. F. Credidio, E. N. Teixeira, S. D. Reis, A. A. Moreira, and J. S. Andrade Jr, *Sci. Rep.* **2**, 920 (2012).
- [22] Michael J. Plank and Edward A. Codling, “Sampling rate and misidentification of lévy and non- lévy movement paths,” *Ecology* **90**, 3546–3553 (2009).
- [23] R. Friedrich, J. Peinke, M. Sahimi, and M. R. R. Tabar, “Approaching complexity by stochastic methods: From biological systems to turbulence,” *Phys. Rep.* **506**, 87–162 (2011).
- [24] L. Rydin Gorjão and F. Meirinhos, “Python KM, a Python package to calculate Kramers–Moyal coeffi-

- cients,” In preparation. Available at <https://github.com/LRydin/KramersMoyal>.
- [25] H. Risken, *The Fokker-Planck Equation*, 2nd ed., Springer Series in Synergetics (Springer, Berlin, 1996).
 - [26] RF Pawula, “Approximation of the linear Boltzmann equation by the Fokker-Planck equation,” *Phys. Rev.* **162**, 186–188 (1967).
 - [27] J. Prusseit and K. Lehnertz, “Stochastic qualifiers of epileptic brain dynamics,” *Phys. Rev. Lett.* **98**, 138103 (2007).
 - [28] K. Lehnertz, “Epilepsy and nonlinear dynamics,” *J. Biol. Phys.* **34**, 253–266 (2008).
 - [29] J. Prusseit and K. Lehnertz, “Measuring interdependences in dissipative dynamical systems with estimated Fokker-Planck coefficients,” *Phys. Rev. E* **77**, 041914 (2008).
 - [30] A.M. van Mourik, A Daffertshofer, and P.J. Beek, “Estimating Kramers-Moyal coefficients in short and non-stationary data sets,” *Phys. Lett. A* **351**, 13–17 (2006).
 - [31] D. Lamouroux and K. Lehnertz, “Kernel-based regression of drift and diffusion coefficients of stochastic processes,” *Phys. Lett. A* **373**, 35073512 (2009).

Appendices

A. EXTENDED DERIVATION OF THE TWO-DIMENSIONAL KRAMERS–MOYAL COEFFICIENTS FOR A JUMP-DIFFUSION PROCESS

The following derivations stem from (3) and apply to the two-dimensional jump-diffusion process (y_1, y_2) , as in (1). All orders of the Kramers–Moyal coefficients $\mathcal{M}^{[\ell, m]}$ are $\ell, m \in \mathbb{N}_+$.

A. Kramers–Moyal coefficients $\mathcal{M}^{[1,0]}$ and $\mathcal{M}^{[0,1]}$

$$\begin{aligned}
\mathcal{M}^{[1,0]}(x_1, x_2) &= \lim_{dt \rightarrow 0} \frac{1}{dt} \langle (dy_1)^1 (dx_2)^0 \rangle |_{y_1(t)=x_1, y_2(t)=x_2} \\
&= \lim_{dt \rightarrow 0} \frac{1}{dt} \langle dy_1 \rangle |_{y_1(t)=x_1, y_2(t)=x_2} \\
&= \lim_{dt \rightarrow 0} \frac{1}{dt} \langle N_1 dt + g_{1,1} dw_1 + g_{1,2} dw_2 + \xi_{1,1} dJ_1 + \xi_{1,2} dJ_2 \rangle |_{y_1(t)=x_1, y_2(t)=x_2} \\
&= \lim_{dt \rightarrow 0} \frac{1}{dt} [N_1 dt + g_{1,1} \langle dw_1 \rangle + g_{1,2} \langle dw_2 \rangle + \langle \xi_{1,1} \rangle \langle dJ_1 \rangle + \langle \xi_{1,2} \rangle \langle dJ_2 \rangle] \\
&= N_1,
\end{aligned}$$

where $\langle g_{i,j} dW_j \rangle = \langle g_{i,j} \rangle \langle dW_j \rangle = 0$, because a Wiener process has the property $\langle dW_j \rangle = 0$. Further $\langle \xi_{i,j} dJ_j \rangle = \langle \xi_{i,j} \rangle \langle dJ_j \rangle = 0$, since $\xi_{i,j}$ is a Gaussian with mean value zero, i.e., $\langle \xi_{i,j} \rangle = 0$. Mutatis mutandis for $\mathcal{M}^{[0,1]}$.

B. Kramers–Moyal coefficient $\mathcal{M}^{[1,1]}$

$$\begin{aligned}
\mathcal{M}^{[1,1]} &= \lim_{dt \rightarrow 0} \frac{1}{dt} \langle (dy_1)^1 (dy_2)^1 \rangle |_{y_1(t)=x_1, y_2(t)=x_2} \\
&= \lim_{dt \rightarrow 0} \frac{1}{dt} \langle (N_1 dt + g_{1,1} dw_1 + g_{1,2} dw_2 + \xi_{1,1} dJ_1 + \xi_{1,2} dJ_2) \cdot \\
&\quad (N_2 dt + g_{2,1} dw_1 + g_{2,2} dw_2 + \xi_{2,1} dJ_1 + \xi_{2,2} dJ_2) \rangle |_{y_1(t)=x_1, y_2(t)=x_2} \\
&= \lim_{dt \rightarrow 0} \left[N_1 N_2 dt + g_{1,1} g_{2,1} \langle (dw_1)^2 \rangle \frac{1}{dt} + g_{1,2} g_{2,2} \langle (dw_2)^2 \rangle \frac{1}{dt} + \mathcal{O}(dt) \right] \\
&= g_{1,1} g_{2,1} + g_{1,2} g_{2,2},
\end{aligned}$$

where higher-order terms $\mathcal{O}(dt)^\epsilon$, with $\epsilon > 0$, vanish in the limit $dt \rightarrow 0$. Recall as well $\langle (dw_i)^2 \rangle = dt$.

C. Kramers–Moyal coefficients $\mathcal{M}^{[2,0]}$ and $\mathcal{M}^{[0,2]}$

$$\begin{aligned}
\mathcal{M}^{[2,0]} &= \lim_{dt \rightarrow 0} \frac{1}{dt} \frac{1}{2!} \langle (dy_1)^2 \rangle |_{y_1(t)=x_1, y_2(t)=x_2} \\
&= \lim_{dt \rightarrow 0} \frac{1}{dt} \frac{1}{2} \langle (N_1 dt + g_{1,1} dw_1 + g_{1,2} dw_2 + \xi_{1,1} dJ_1 + \xi_{1,2} dJ_2)^2 \rangle |_{y_1(t)=x_1, y_2(t)=x_2} \\
&= \lim_{dt \rightarrow 0} \frac{1}{2} \left[N_1^2 dt + g_{1,1}^2 \langle (dw_1)^2 \rangle \frac{1}{dt} + g_{1,2}^2 \langle (dw_2)^2 \rangle \frac{1}{dt} + \langle \xi_{1,1}^2 \rangle \langle (dJ_1)^2 \rangle \frac{1}{dt} + \right. \\
&\quad \left. \langle \xi_{1,2}^2 \rangle \langle (dJ_2)^2 \rangle \frac{1}{dt} + \mathcal{O}(dt) \right] \\
&= \frac{1}{2} [g_{1,1}^2 + s_{1,1} \lambda_1 + g_{1,2}^2 + s_{1,2} \lambda_2],
\end{aligned}$$

Using the previously employed nomenclature $\langle \xi_{ij}^2 \rangle = \sigma_{\xi_{ij}}^2 = s_{ij}$ as well as $\langle (dJ_i)^2 \rangle = \lambda_i dt$. Mutatis mutandis for $\mathcal{M}^{[0,2]}$

$$\mathcal{M}^{[0,2]} = \frac{1}{2} [g_{2,1}^2 + s_{2,1}\lambda_1 + g_{2,2}^2 + s_{2,2}\lambda_2],$$

D. Kramers–Moyal coefficient $\mathcal{M}^{[2,2]}$

$$\begin{aligned} \mathcal{M}^{[2,2]} &= \lim_{dt \rightarrow 0} \frac{1}{dt} \langle (dy_1)^2 (dy_2)^2 \rangle |_{y_1(t)=x_1, y_2(t)=x_2} \\ &= \lim_{dt \rightarrow 0} \frac{1}{dt} \langle (N_1 dt + g_{1,1} dw_1 + g_{1,2} dw_2 + \xi_{1,1} dJ_1 + \xi_{1,2} dJ_2)^2 \cdot \\ &\quad (N_2 dt + g_{2,1} dw_1 + g_{2,2} dw_2 + \xi_{2,1} dJ_1 + \xi_{2,2} dJ_2)^2 \rangle |_{y_1(t)=x_1, y_2(t)=x_2} \\ &= \lim_{dt \rightarrow 0} \frac{1}{dt} \left[\text{terms}(N_1, N_2, \mathcal{O}(dt^4)) + \text{terms}(g_{ij}, \mathcal{O}(dt^2)) + \text{terms}(\text{mixing } \xi_{ij}) + \right. \\ &\quad \langle \xi_{1,1}^2 \rangle \langle \xi_{2,1}^2 \rangle \langle (dJ_1)^4 \rangle + \langle \xi_{1,2}^2 \rangle \langle \xi_{2,2}^2 \rangle \langle (dJ_2)^4 \rangle + \\ &\quad \left. \langle \xi_{1,1}^2 \rangle \langle \xi_{2,2}^2 \rangle \langle (dJ_1)^2 \rangle \langle (dJ_2)^2 \rangle + \langle \xi_{1,2}^2 \rangle \langle \xi_{2,1}^2 \rangle \langle (dJ_1)^2 \rangle \langle (dJ_2)^2 \rangle \right] \\ &= s_{1,1} s_{2,1} \lambda_1 + s_{1,2} s_{2,2} \lambda_2. \end{aligned}$$

Terms including dt on the right-hand side of the above equation vanish as for $dt \rightarrow 0$, where as well $\langle \xi_{1,1} \xi_{1,2} \rangle = \langle \xi_{1,1} \rangle \langle \xi_{1,2} \rangle = 0$, and $\frac{1}{dt} [\langle (dJ_1)^2 \rangle \langle (dJ_2)^2 \rangle] = \frac{1}{dt} [\lambda_1 dt \lambda_2 dt] \propto dt$ vanishes in the limit $dt \rightarrow 0$.

E. Kramers–Moyal coefficients $\mathcal{M}^{[\ell,m]}$, for $2 \times (\ell, m) \geq 2$

For $(2\ell, 2m)$, with $(\ell, m) \geq 4$, the Kramers–Moyal coefficients $\mathcal{M}^{[2\ell, 2m]}$ are as follows

$$\begin{aligned} \mathcal{M}^{[2\ell, 2m]} &= \lim_{dt \rightarrow 0} \frac{1}{dt} \binom{\ell}{m} \langle (dy_1)^{2\ell} (dy_2)^{2m} \rangle |_{y_1(t)=x_1, y_2(t)=x_2} \\ &= \lim_{dt \rightarrow 0} \frac{1}{dt} \binom{\ell}{m} \langle (N_1 dt + g_{1,1} dw_1 + g_{1,2} dw_2 + \xi_{1,1} dJ_1 + \xi_{1,2} dJ_2)^{2\ell} \cdot \\ &\quad (N_2 dt + g_{2,1} dw_1 + g_{2,2} dw_2 + \xi_{2,1} dJ_1 + \xi_{2,2} dJ_2)^{2m} \rangle |_{y_1(t)=x_1, y_2(t)=x_2} \\ &= \lim_{dt \rightarrow 0} \frac{1}{dt} \binom{\ell}{m} \left[\langle \xi_{1,1}^{2\ell} \rangle \langle \xi_{2,1}^{2m} \rangle \langle (dJ_1)^{2(\ell+m)} \rangle + \langle \xi_{1,2}^{2\ell} \rangle \langle \xi_{2,2}^{2m} \rangle \langle (dJ_2)^{2(\ell+m)} \rangle \right] \\ &= \binom{\ell}{m} [\langle \xi_{1,1}^{2\ell} \rangle \langle \xi_{2,1}^{2m} \rangle \lambda_1 + \langle \xi_{1,2}^{2\ell} \rangle \langle \xi_{2,2}^{2m} \rangle \lambda_2] \\ &= \binom{\ell}{m} \frac{(2\ell)! (2m)!}{2^\ell \ell! 2^m m!} [s_{1,1}^\ell s_{2,1}^m \lambda_1 + s_{1,2}^\ell s_{2,2}^m \lambda_2]. \end{aligned}$$

In the last step, take the fact that the jump amplitudes $\xi_{i,j}$ are Gaussian distributed, thus $\langle \xi_{i,j}^{2\ell} \rangle \propto \sigma_{\xi_{i,j}}^{2\ell} = s_{i,j}^\ell$. In this manner, all Kramers–Moyal coefficients $\mathcal{M}^{[2\ell, 2m]}$, with $(\ell, m) \geq 1$ are obtained.

B. EXTENDED RESULTS FOR MODELLED DATA BY (15)

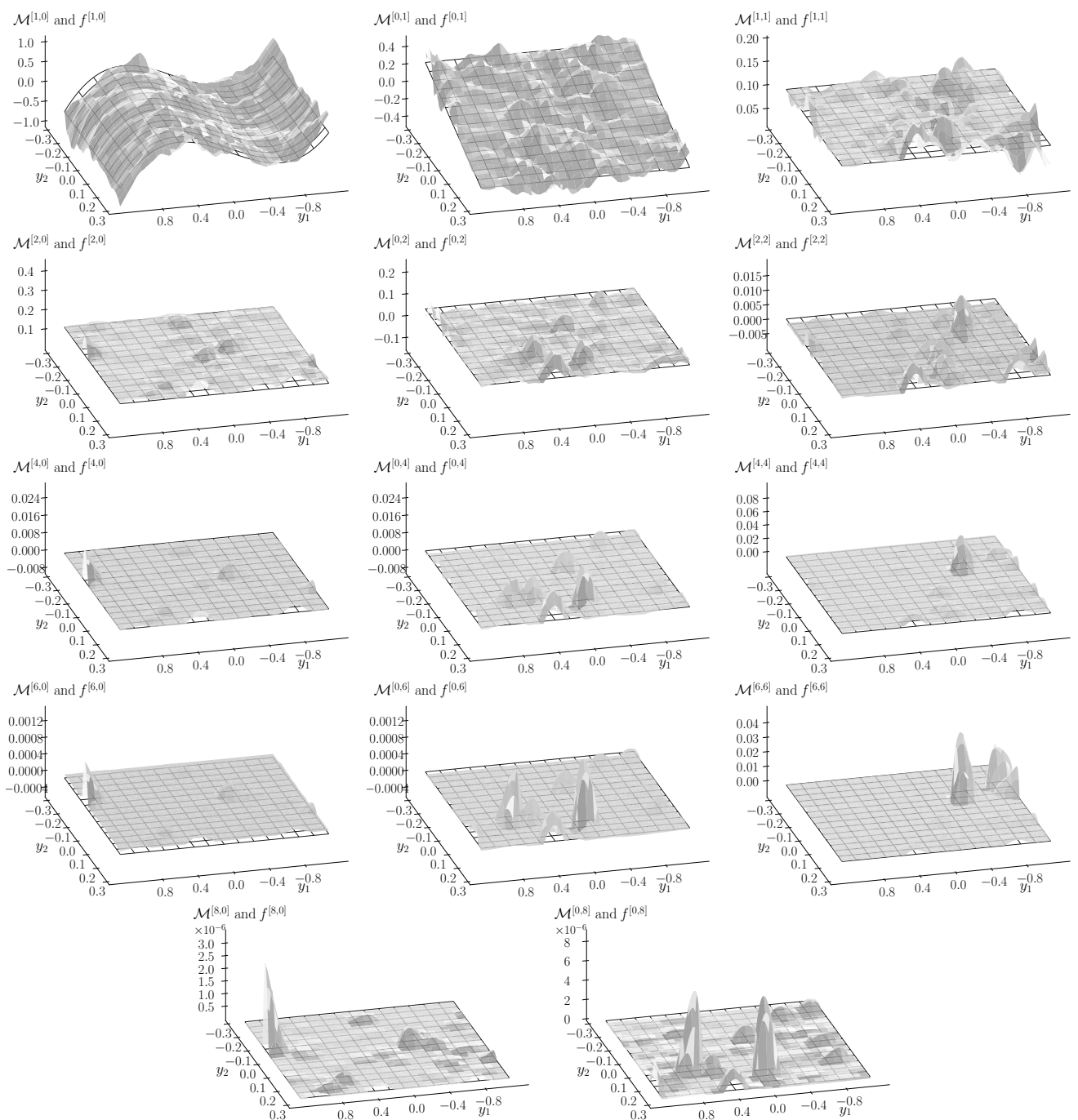


FIG. 9. Two-dimensional Kramers–Moyal coefficients of a bivariate jump-diffusion processes given by (15) and all theoretical expected functions f associated with each Kramers–Moyal coefficient, according to (10), (11), and (12). Exhibited are the Kramers–Moyal coefficients $\mathcal{M}^{[1,0]}$, $\mathcal{M}^{[0,1]}$, $\mathcal{M}^{[1,1]}$, $\mathcal{M}^{[2,0]}$, $\mathcal{M}^{[0,2]}$, $\mathcal{M}^{[2,2]}$, $\mathcal{M}^{[4,0]}$, $\mathcal{M}^{[0,4]}$, $\mathcal{M}^{[4,4]}$, $\mathcal{M}^{[6,0]}$, $\mathcal{M}^{[0,6]}$, $\mathcal{M}^{[6,6]}$, $\mathcal{M}^{[8,0]}$, and $\mathcal{M}^{[0,8]}$. The error volume for the displayed Kramers–Moyal coefficients are: $V_{\text{err}}^{[1,0]} = 0.6836$, $V_{\text{err}}^{[0,1]} = 0.2259$, $V_{\text{err}}^{[1,1]} = 0.0098$, $V_{\text{err}}^{[2,0]} = 0.0144$, $V_{\text{err}}^{[0,2]} = 0.0256$, $V_{\text{err}}^{[2,2]} = 0.0046$, $V_{\text{err}}^{[4,0]} = 0.0148$, $V_{\text{err}}^{[0,4]} = 0.0338$, $V_{\text{err}}^{[4,4]} = 0.0035$, $V_{\text{err}}^{[6,0]} = 0.0217$, $V_{\text{err}}^{[0,6]} = 0.0848$, $V_{\text{err}}^{[6,6]} = 0.0054$, $V_{\text{err}}^{[8,0]} = 0.0374$, $V_{\text{err}}^{[0,8]} = 0.2643$